# Coupled Magneto-Mechanical Analysis of Iron Sheets Under Biaxial Stress

U. Aydin[1], P. Rasilo[1,2], D. Singh[1], A. Lehikoinen[1], A. Belahcen[1] and A. Arkkio[1]

[1]Department of Electrical Engineering and Automation, Aalto University, Espoo, Finland
[2]Department of Electrical Engineering, Tampere University of Technology, Tampere, Finland

**A novel single sheet tester design is proposed and a directly coupled magneto-mechanical model is used to numerically analyze the behavior of iron sheets under biaxial magneto-mechanical loading applied by the tester device. Magneto-mechanically coupled constitutive equations of the material derived using an energy based approach are integrated into a finite element model of the single sheet tester device and simulations are performed to solve for the displacement field and the magnetic vector potential in the sample. The obtained numerical results of magnetostriction evolution due to uniaxial stress and stress induced anisotropies due to permeability variation under different magneto-mechanical loadings are presented. The simulation results are compared to the results published in the literature for the purpose of validation.**

*Index Terms*—**Inverse magnetostriction, magnetoelasticity, magnetomechanical effects, magnetostriction, strain, stress.**

## I. Introduction

MAGNETOSTRICTION (MS) is a phenomenon in ferromagnetic materials which causes strain in the presence of magnetic fields. This effect is known to be a source of acoustic noise in electrical machines [1]-[2]. Another phenomenon which is called inverse magnetostriction (IM) causes permeability variation in the ferromagnetic materials when subjected to stress. Due to IM, performance of electromagnetic devices is affected [3]-[4].

In most electromagnetic applications devices are subjected to multi-axial stresses. These stresses can be caused due to manufacturing processes and/or during their operation. The orientation of stress in the materials with respect to the magnetic field may also vary. This multi-axiality of magneto-mechanical loadings points out the need for characterization of the ferromagnetic materials under complex magneto-mechanical loadings. Several studies were performed in order to measure the effects of the biaxial magneto-mechanical loadings on the ferromagnetic materials [5]-[7]. However, these test setups do not provide control for obtaining arbitrary in-plane stress tensor in the test material as it occurs in the operation of, for instance, rotational electrical machines [5]. On the other hand, some research has been done on modeling of the coupled multi-axial magneto-mechanical behavior [8]-[10]. Some measurements are often made to obtain necessary material data during modeling process as in [8]-[9]. A different approach is taken in [10] by defining a local free energy in domain scale and obtaining macroscopic magneto-elastic behavior by homogenization of local behavior.

In this paper a novel single sheet tester device design is proposed and a coupled magneto-mechanical model of the tester device is developed using an energy based directly coupled model for magneto-elastic deformation. The implementation of the model to the finite element method (FEM) of the device is performed in order to numerically analyze the coupled magneto-mechanical properties of the studied material and applicability of the device for multi-axial magneto-mechanical measurements of the electrical sheets. Obtained magneto-mechanical behavior of the studied material that is consistent with experimental measurements and modeling results from the literature is presented.

Manuscript received July 2, 2015; revised September 30, 2015; accepted October 27, 2015. Date of publication Xxxxxxxxx xx, xxxx; date of current version Xxxxxxxxx xx, xxxx. Corresponding author: U. Aydin. (e-mail: ugur.aydin@aalto.fi).

Color versions of one or more of the figures in this paper are available online at http://ieeexplore.ieee.org.

Digital Object Identifier (inserted by IEEE).

## II. Method

Based on [11] and [12] constitutive equations for coupling the magnetic and elastic properties of the material are derived from a Helmholtz free energy density $\psi$. In case of a magneto-elastic material this energy is a function of magnetic flux density $\boldsymbol{B}$ and strain tensor $\boldsymbol{\varepsilon}$ and can be expressed by using the following five invariants as $\psi(I_1, I_2, I_4, I_5, I_6)$:

$$I_1 = \mathrm{tr}\boldsymbol{\varepsilon}, \quad I_2 = \frac{1}{2}\mathrm{tr}\boldsymbol{\varepsilon}^2$$
$$I_4 = \boldsymbol{B}\cdot\boldsymbol{B}, \quad I_5 = \boldsymbol{B}\cdot(\tilde{\boldsymbol{\varepsilon}}\boldsymbol{B}), \quad I_6 = \boldsymbol{B}\cdot(\tilde{\boldsymbol{\varepsilon}}^2\boldsymbol{B}). \tag{1}$$

Because linear elasticity is assumed, $\psi$ does not depend on the third invariant $I_3$ which is not given in (1). The first two invariants describe the elastic behavior of the material. The fourth invariant is chosen to describe the single-valued magnetization behavior, whereas the fifth and sixth invariants determine the MS response. Since the permeability variation is independent from hydrostatic pressure, in the fifth and sixth invariants the deviatoric part of the strain $\tilde{\boldsymbol{\varepsilon}}$ is used. The Helmholtz free energy density function $\psi$ given in [11] is modified slightly and written as

$$\psi = \frac{1}{2}\lambda I_1^2 + 2GI_2 + \sum_{i=0}^{n_\alpha-1}\frac{g_i(I_1)}{i+1}I_4^{i+1} + \sum_{i=0}^{n_\beta-1}\beta_i I_5 + \sum_{i=0}^{n_\gamma-1}\gamma_i I_6 \tag{2}$$

This article has been accepted for publication in a future issue of this journal, but has not been fully edited. Content may change prior to final publication. Citation information: DOI 10.1109/TMAG.2015.2496207, IEEE Transactions on Magnetics



where the function

$$g_i(I_1)=\alpha_i \exp\left(\frac{4(i+1)}{3}I_1\right)-\begin{cases}\frac{\nu_0}{8}, & \text{if } i=0\\ 0, & \text{if } i>0\end{cases} \quad (3)$$

is derived so as to obtain isochoric MS under purely magnetic loading [11]. $\nu_0$ is the reluctivity of free space, $\alpha_i$, $\beta_i$ and $\gamma_i$ are fitting parameters, whereas $\lambda$ and $G$ are the Lamé parameters. In (2) first two terms account for purely mechanical behavior, and the last three terms account for the magneto-mechanical coupling. The summation term in the middle accounts for non-linear $\boldsymbol{H}(\boldsymbol{B},\boldsymbol{\varepsilon})$ relationship. In this work $\nu_0/8$ term is removed from $g_i$ to have better convergence in numerical analysis under multiaxial loadings. This causes deviation from isochoric MS with magnitude of approximately 1.2 μm/m under 1 T $\boldsymbol{B}$ and it has to be noted as a limitation of this model.

Using the Helmholtz free energy density and the chain rule of derivative, the constitutive equations for the magneto-elastic stress tensor $\boldsymbol{\sigma}_{\text{me}}$ and the magnetic field strength vector $\boldsymbol{H}$ can be expressed as

$$\boldsymbol{\sigma}_{\text{me}}=\rho\sum_{i=1,i\neq3}^{6}\frac{\partial\psi}{\partial I_i}\frac{\partial I_i}{\partial\boldsymbol{\varepsilon}} \quad \text{and} \quad \boldsymbol{H}=\rho\sum_{i=1,i\neq3}^{6}\frac{\partial\psi}{\partial I_i}\frac{\partial I_i}{\partial\boldsymbol{B}} \quad (4)$$

where $\rho$ is the mass density. The magnetization vector $\boldsymbol{M}$ depends on $\boldsymbol{B}$ as $\boldsymbol{M}=\nu_0\boldsymbol{B}-\boldsymbol{H}$. The magneto-elastic stress tensor $\boldsymbol{\sigma}_{\text{me}}$ consists of elastic stress and MS related stress tensors. Total electromagnetic forces acting on the iron known as Maxwell stress tensor $\boldsymbol{\sigma}_{\text{mag}}$ and given by

$$\boldsymbol{\sigma}_{\text{mag}}=\nu_0\boldsymbol{B}\boldsymbol{B}-\boldsymbol{B}\boldsymbol{M}-\frac{1}{2}\nu_0(\boldsymbol{B}\cdot\boldsymbol{B})\boldsymbol{I}+(\boldsymbol{B}\cdot\boldsymbol{M})\boldsymbol{I} \quad (5)$$

where $\boldsymbol{I}$ is the identity tensor [13]. The total stress tensor $\boldsymbol{\sigma}$ is expressed as the sum of $\boldsymbol{\sigma}_{\text{mag}}$ and $\boldsymbol{\sigma}_{\text{me}}$ as

$$\boldsymbol{\sigma}(\boldsymbol{B},\boldsymbol{\varepsilon})=\boldsymbol{\sigma}_{\text{me}}(\boldsymbol{B},\boldsymbol{\varepsilon})+\boldsymbol{\sigma}_{\text{mag}}(\boldsymbol{B},\boldsymbol{\varepsilon}). \quad (6)$$

Using the balance equations for magneto-elastic solids while taking into account external mechanical forces $\boldsymbol{f}_{\text{mec}}$ and assuming there are no current sources in iron we obtain

$$-\nabla\cdot\boldsymbol{\sigma}=\boldsymbol{f}_{\text{mec}} \quad (7)$$

$$\nabla\times\boldsymbol{H}=0. \quad (8)$$

In order to solve the coupled problem using FEM for displacements $\boldsymbol{u}$ and the nodal values of the magnetic vector potential $\boldsymbol{A}$ the Galerkin weighted residual weak form is applied to (7) and (8). Afterwards discretization is applied by using the nodal basis functions for $\boldsymbol{u}$ and $\boldsymbol{A}$. The obtained non-linear system can be solved by Newton-Raphson method iteratively. The detailed implementation of the model to the FEM can be found in [11] and [12]. The strain and the magnetic flux density are then obtained as

$$\boldsymbol{\varepsilon}=\frac{1}{2}(\nabla\boldsymbol{u}+\nabla\boldsymbol{u}^{\text{T}}) \quad (9)$$

$$\boldsymbol{B}=\nabla\times\boldsymbol{A}. \quad (10)$$

## III. Identification of Model

Fifteen parameters which are given in Table I are needed to model the properties of the studied material, 0.5 mm non-oriented Si-Fe sheets, and they were determined using experimental data obtained from a custom built uniaxial single sheet tester [14]. In the experiment process the material was loaded with different stresses varying from 50 MPa compression (–) to 80 MPa tension (+) parallel to the flux density and magnetization curves were measured. Afterwards, initial fitting of the single valued model parameters to the $\boldsymbol{H}$-averaged measured magnetization loops was realized at various stress values as shown in Fig. 1.

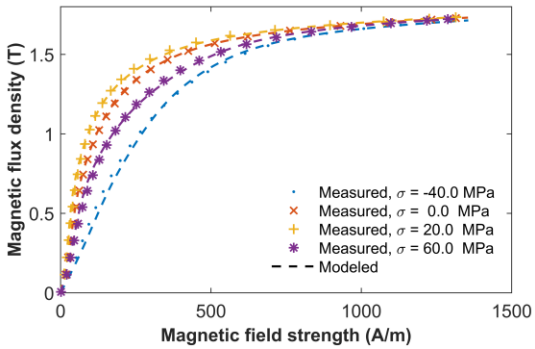


Fig. 1. Fitting results of single valued model parameters to $\boldsymbol{H}$-averaged magnetization curve measurements.

TABLE I
PARAMETER VALUES USED IN THE MODEL

| Param. | Value | Param. | Value | Param. | Value |
|---|---|---|---|---|---|
| $\alpha_0$ | $7.3\cdot10^{-5}$ | $\alpha_5$ | –13.709 | $\beta_2$ | –4.798 |
| $\alpha_1$ | –97.030 | $\alpha_6$ | –6.202 | $\beta_3$ | $-1.3\cdot10^{3}$ |
| $\alpha_2$ | 250.427 | $\alpha_7$ | 1.589 | $\gamma_0$ | 1.178 |
| $\alpha_3$ | –250.520 | $\beta_0$ | –0.283 | $\gamma_1$ | 1.059 |
| $\alpha_4$ | 117.438 | $\beta_1$ | –1.872 | $\gamma_2$ | 58.230 |

Magnetic materials show reduced permeability under compression and high tension. This behavior of magnetic materials is modeled successfully using the model. Besides, increased permeability is observed under low tensile stress as reported in [14].

## IV. Applications and Results

### A. Novel Biaxial Single Sheet Tester Design

The presented model is implemented to a FEM model of a novel biaxial single sheet tester device to numerically analyze the effect of more complex stress states on the magnetic properties of the studied material. Fig. 2 (a) shows the design of the tester device. Setup is designed so as to analyze

This article has been accepted for publication in a future issue of this journal, but has not been fully edited. Content may change prior to final publication. Citation information: DOI 10.1109/TMAG.2015.2496207, IEEE Transactions on Magnetics



magneto-mechanical properties of studied material by obtaining arbitrary flux density and in-plane stress tensor in the central area $C_0$ of the sample. This will be done by magnetizing the sample by six coils which are placed around the magnetizing yoke and applying suitable mechanical loadings to the six arms of the sample in pairs $L_{0°}$, $L_{60°}$, $L_{120°}$. Excitation voltage of the coils can be controlled by using the procedure explained in [15]. The homogeneity of the magnetic field and the stress in the central region is tested under purely magnetic and mechanical loading numerically using FEM model of the device. Maximum variations of the magnetic field and the stress in 400 mm$^2$ area in the central region are found to be 7% and 15%, respectively. Magnetic flux density and *y*-component of the stress tensor distribution in the central region are shown in Fig. 2. (b) for a single simulation.

In order to have desired in-plane stress tensor at the point $C_0$ the required mechanical loadings for each arm pair can be calculated by constructing a linear set of equations since a linear elastic material is assumed. The procedure is following:

1. A reference mechanical pressure $p_{\text{ref}}$ is applied only to the $L_0$ arm pair of the non-magnetized sample and a finite element (FE) simulation is performed to obtain a reference in-plane stress tensor as

$$\boldsymbol{\sigma}_{\text{ref},\theta} = \begin{bmatrix} \sigma_{\text{ref},\theta\text{xx}} & \sigma_{\text{ref},\theta\text{xy}} \\ \sigma_{\text{ref},\theta\text{xy}} & \sigma_{\text{ref},\theta\text{yy}} \end{bmatrix}\Bigg|_{\theta=0°} \tag{11}$$

2. A coordinate transformation is applied using coordinate transformation matrix $Q_\theta$ for angles 60° and 120° degrees to get reference stress tensors for arms $L_{60°}$ and $L_{120°}$ in the central point $C_0$ as

$$Q_\theta = \begin{bmatrix} \cos\theta & \sin\theta \\ -\sin\theta & \cos\theta \end{bmatrix} \tag{12}$$

$$\boldsymbol{\sigma}_{\text{ref},\theta} = Q_\theta \cdot \boldsymbol{\sigma}_{\text{ref},0} \cdot Q_\theta^{\text{T}}\Big|_{\theta=60°,120°} \tag{13}$$

3. Let us define required unknown loadings to be applied to the arms $L_{0°}$, $L_{60°}$, $L_{120°}$ to obtain desired in-plane stress tensor $\boldsymbol{\sigma}'$ in the point $C_0$ as $p_{0°}$, $p_{60°}$, $p_{120°}$, respectively. Since linear elasticity is assumed a linear relation between $p_{0°}$, $p_{60°}$, $p_{120°}$ and $p_{\text{ref}}$ can be used to set following equation

$$\boldsymbol{\sigma}' = \boldsymbol{\sigma}_{\text{ref},0°} \cdot \frac{p_{0°}}{p_{\text{ref}}} + \boldsymbol{\sigma}_{\text{ref},60°} \cdot \frac{p_{60°}}{p_{\text{ref}}} + \boldsymbol{\sigma}_{\text{ref},120°} \cdot \frac{p_{120°}}{p_{\text{ref}}}. \tag{14}$$

Equation (14) can be written in more clear form as

$$\begin{bmatrix} \sigma'_{\text{xx}} \\ \sigma'_{\text{yy}} \\ \sigma'_{\text{xy}} \end{bmatrix} = \frac{1}{p_{\text{ref}}} \cdot \begin{bmatrix} \sigma_{\text{ref},0°\text{xx}} & \sigma_{\text{ref},60°\text{xx}} & \sigma_{\text{ref},120°\text{xx}} \\ \sigma_{\text{ref},0°\text{yy}} & \sigma_{\text{ref},60°\text{yy}} & \sigma_{\text{ref},120°\text{yy}} \\ \sigma_{\text{ref},0°\text{xy}} & \sigma_{\text{ref},60°\text{xy}} & \sigma_{\text{ref},120°\text{xy}} \end{bmatrix} \cdot \begin{bmatrix} p_{0°} \\ p_{60°} \\ p_{120°} \end{bmatrix}. \tag{15}$$

Solution of this system for $p_{0°}$, $p_{60°}$, and $p_{120°}$ yields the required loading values that need to be applied to the arm pairs $L_{0°}$, $L_{60°}$, and $L_{120°}$ in order to have arbitrary in-plane stress tensor $\boldsymbol{\sigma}'$ in the central point $C_0$.

The presented procedure is sensitive to the meshing of the device geometry when performing the FE simulation in the first step. The arm pairs and the corresponding region in the central area should have symmetrical meshes with respect to each other.

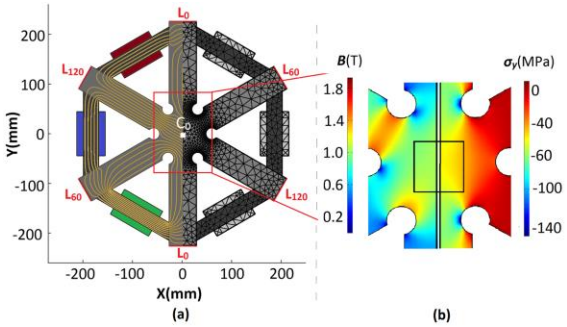


Fig. 2. (a) Biaxial single sheet tester design geometry. On the left side magnetized sample without any mechanical loading and on the right side meshed geometry is presented. (b) Static single FE simulation results for magnetic flux density (left) and *y*-component of stress distribution (right).

### B. *Effect of Various Stress States on Magnetic Properties*

Using the mentioned procedure any in-plane stress state can be obtained in the point $C_0$. The studied stress tensors in this work are

$$\boldsymbol{\sigma}_{\text{uni}} = \begin{bmatrix} 0 & 0 \\ 0 & \sigma \end{bmatrix}, \quad \boldsymbol{\sigma}_{\text{equ}} = \begin{bmatrix} \sigma & 0 \\ 0 & \sigma \end{bmatrix}, \quad \boldsymbol{\sigma}_{\text{shear}} = \begin{bmatrix} \sigma & 0 \\ 0 & -\sigma \end{bmatrix} \tag{16}$$

where $\boldsymbol{\sigma}_{\text{uni}}$, $\boldsymbol{\sigma}_{\text{equ}}$ and $\boldsymbol{\sigma}_{\text{shear}}$ are uniaxial, equibiaxial and pure shear stress states, respectively. First, several static FE simulations are performed where the sample is magnetized along the *y*-axis and suitable mechanical loadings are applied to the arms of the sample to obtain uniaxial stress distribution $\boldsymbol{\sigma}_{\text{uni}}$ in the point $C_0$ at different magnitudes. Maxwell's stress tensor (5) is not considered in the surrounding air domain. The MS response parallel to magnetization direction under uniaxial stress is shown in Fig. 3 (a). Compression increases the MS, whereas tensile stress tends to decrease it [10],[12],[16].

In order to see the effect of more complex stress states FE simulations are performed under mechanical loadings that are given in (16) and rotational $\boldsymbol{B}$. To obtain a circular $\boldsymbol{B}$ with magnitude of 1 T in the center point, controlled vector potential boundary conditions are imposed to the arms of the sample. Fig. 4 (a) shows the rate of change of the flux in one arm, which corresponds to the electromotive force in coils under different stress states and levels. This result shows the need of consideration for the effect of stresses on the excitation voltage waveform control in practice. Fig. 4 (b), (c) and (d) give the locus of $\boldsymbol{H}$ under afore mentioned $\boldsymbol{B}$ in the center point $C_0$ of the sample and under zero stress, uniaxial, equibiaxial and pure shear stress states, respectively. Since isotropic material is assumed, the locus of $\boldsymbol{H}$ is circular under zero stress. Stress induced anisotropy is clearly seen under

This article has been accepted for publication in a future issue of this journal, but has not been fully edited. Content may change prior to final publication. Citation information: DOI 10.1109/TMAG.2015.2496207, IEEE Transactions on Magnetics



external mechanical loading. For instance, considering 20 MPa uniaxial tensile stress the major principal plane direction of the applied stress becomes an easy direction whereas the minor principal plane direction becomes a hard direction for magnetization. Opposite effect is seen in uniaxial compressive stress since it deteriorates the permeability on the major plane direction. Considering the applied stress magnitudes another important point is that the least effect on permeability is caused by equibiaxial stress. On the other hand, pure shear stress state induces highest anisotropy in the material. Even though different materials are studied, the modeled behavior under various mechanical loadings including biaxial ones and rotational magnetization is in agreement with the experimental measurements from [6] and modeling results from [3].

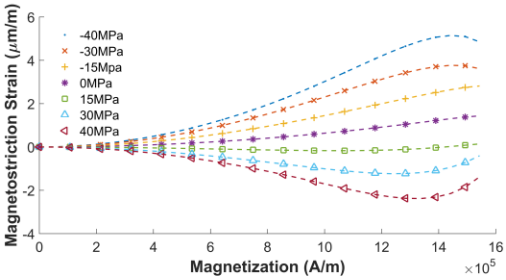


Fig. 3. MS response parallel to the magnetization direction under uniaxial stress compression and tension.

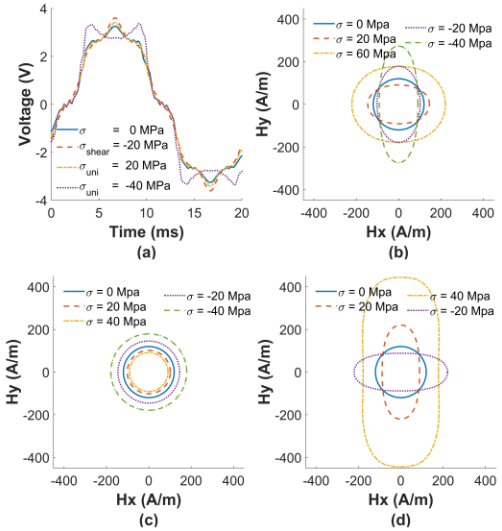


Fig. 4. Corresponding voltage waveforms in coils that are obtained from boundary conditions and locus of $\boldsymbol{H}$ under different stress states and magnitudes (a) Evolution of the voltage waveforms under different stress states and magnitudes. (b), (c) and (d) Resulting $\boldsymbol{H}$ locus under uniaxial, equibiaxial and pure shear stress states with different magnitudes.

## V. Conclusion

A novel single sheet tester device design is proposed and a strongly coupled magneto-mechanical model which is identified only from stress dependent anhysteretic $\boldsymbol{B}$-$\boldsymbol{H}$ curves was implemented to FEM model of the tester device. The magneto-mechanical behavior of the device and the effect of multiaxial stress on magnetic behavior of iron sheets are analyzed using the model. It was shown that with the tester device it is possible to obtain uniform field distribution and any desired in-plane stress tensor in the center point of the sample sheet by applying suitable mechanical loadings. This allows comprehensive magneto-mechanical analysis of the studied material. Several stress states including multiaxial ones were applied to the device which was magnetized by rotational magnetic field. Results are promising and consistent with the experimental and modeling results from literature.

## VI. Acknowledgement

The research leading to these results has received funding from European Research Council under the European Union's Seventh Framework Programme (FP7/2007-2013) / ERC grant agreement n°339380. P. Rasilo acknowledges the Academy of Finland for financial support.

## References

[1] B. Weiser, H. Pfützner, and J. Anger, "Relevance of magnetostriction and forces for the generation of audible noise of transformer cores," *IEEE Trans. Magn.*, vol. 36, pp. 3759–3777, Sep. 2000.

[2] O. A. Mohammed, T. E. Calvert, L. Petersen, and R. McConnell, "Transient Modeling of Coupled Magnetoelastic Problems in Electrical Machines," *IEEE Pow. Eng. Soc. Summer Meeting*, vol. 1, pp. 281–287, Jul. 2002.

[3] L. Bernard, and L. Daniel, "Effect of Stress on Magnetic Hysteresis Losses in a Switched Reluctance Motor: Application to Stator and Rotor Shrink Fitting," *IEEE Trans. Magn.*, vol. 51, no. 9, pp. 7002513, Sep. 2015.

[4] O. A. Mohammed, S. C. Ganu, and S. Liu, "FEM Analysis and Testing of Magnetostrictive Effects in Electrical Steel Samples For Machinery Applications," *IEEE Pow. Eng. Soc. General Meeting*, vol. 3, pp. 1496–1500, Jul. 2003.

[5] M. Rekik, O. Hubert, and L. Daniel, "Influence of a multiaxial stress on the reversible and irreversible magnetic behaviour of a 3%Si-Fe alloy," *Int. Jour. of Appl. Electromagnetics and Mechanics*, vol. 44, no. 3–4, pp. 301–315, Mar. 2014.

[6] Y. Kai, Y. Tsuchida, T. Todaka, and M. Enokizono, "Influence of Biaxial Stress on Vector Magnetic Properties and 2-D Magnetostriction of a Nonoriented Electrical Steel Sheet under Alternating Magnetic Flux Conditions," *IEEE Trans. Magn.*, vol. 50, no. 4, pp. 6100204, Apr. 2014.

[7] J. Pearson, P. T. Squire, M. G. Maylin, and J. G. Gore, "Apparatus for Magnetic Measurements Under Biaxial Stress," *IEEE Trans. Magn.*, vol. 36, no. 5, pp. 3599–3601, Sept. 2000.

[8] H. Ebrahimi, Y. Gao, H. Dozono, and K. Muramatsu, "Coupled Magneto-Mechanical Analysis in Isotropic Materials Under Multiaxial Stress," *IEEE Trans. Magn.*, vol. 50, no. 2 pp. 7006904, Feb. 2014.

[9] O. A. Mohammed, "Coupled magnetoelastic finite element formulation including anisotropic reluctivity tensor and magnetostriction effects for machinery applications," *IEEE Trans. Magn.*, vol. 37, no. 5, pp. 3388–3392, Sep. 2001.

[10] O. Hubert, L. Daniel, "Energetical and multiscale approaches for the definition of an equivalent stress for magneto-elastic couplings," *Jour. of Magn. and Magn. Mat.*, vol. 323, iss. 13, pp. 1766–1781, Jul. 2011.

[11] K. Fonteyn, "Energy-Based Magneto-Mechanical Model for Electrical Steel Sheets," Ph.D. thesis, Aalto University, Espoo, Finland, 2010.

[12] K. Fonteyn, A. Belahcen, R. Kouhia, P. Rasilo, and A. Arkkio, "FEM for Directly Coupled Magneto-Mechanical Phenomena in Electrical Machines," *IEEE Trans. Magn.*, vol. 46, no. 8, pp. 2923–2926, Aug. 2010.

[13] A. Kovetz, "Electromagnetic Theory," *Oxford University Press*, 2000.

[14] D. Singh, P. Rasilo, F. Martin, A. Belahcen, and A. Arkkio, "Effect of Mechanical Stress on Excess Loss of Electrical Steel Sheets," *IEEE Trans. Magn*, In Press.

[15] S. Zurek, P. Marketos, T. Meydan, and A. J. Moses, "Use of Novel Adaptive Digital Feedback for Magnetic Measurements Under Controlled Magnetizing Conditions," *IEEE Trans. Magn.*, vol. 41, no. 11, Nov. 2005.

[16] L. Daniel, M. Rekik, O. Hubert, "A multiscale model for magneto-elastic behaviour including hysteresis effect," *Archive of Appl. Mech.*, vol. 84, issue 9, pp. 1307–1323 May 2014.